Consideration on the Metachromatic Spectra of Toluidine Blue Dimers Formed on DNA Oligomers

Saori Sato,[1] **Shinya Matsumoto,**[*2] **Talivaldis Freivalds,**[3] **and Jekaterina Erenpreisa**[3]

[1]Department of Environment and Natural Sciences, Graduate School of Environment and Information Sciences, Yokohama National University, 79-7 Tokiwadai, Hodogaya-ku, Yokohama 240-8501

[2]Department of Environmental Sciences, Faculty of Education and Human Sciences, Yokohama National University, 79-2 Tokiwadai, Hodogaya-ku, Yokohama 240-8501

[3]Biomedical Research and Study Center, University of Latvia, Ratsupites 1, LV 1067 Riga, Latvia

Received February 8, 2010; E-mail: smatsu@edhs.ynu.ac.jp

Metachromatic staining with toluidine blue (TB) has been used as a cytological tool for tissue recognition and cancer diagnosis. Recently, its strong potential for infertility diagnosis was also reported. Metachromatic staining is important in biological applications, but the origin of spectral changes has not been fully understood, although dye aggregation on biological materials is thought to be the cause. In this study, we investigated the dimer structure of TB formed on DNA oligomers by using a computational method, particularly focusing on the spectral changes caused by TB dimer formation. The structure of the TB–DNA complexes was constructed on the basis of the calculated molecular structure of TB and crystal data of A- and B-form DNA oligomers, assuming that there was an electrostatic interaction between them. The resulting spectral shift was then evaluated using the extended-dipole model. The examination of B-DNA revealed that possible TB dimers result in a hypsochromic spectral shift of absorption. On the other hand, the dimerization of TB on A-DNA was found to be quite difficult, because the helical geometry of A-DNA restricted the binding sites of TB. These results suggest that the metachromatic color observed during biological staining is significantly affected by the helical geometry of DNA.

Toluidine blue (TB) (Figure 1) is an important cationic dye in biological staining, because of its metachromatic effect. Metachromasy is a color change that dyes exhibit when bound to particular biological macromolecules or when concentrated in solution.[1] This characteristic makes it possible to stain certain tissue elements in different colors using a single dye. TB, for instance, stains the granules of mast cells and small oral cancers with the metachromatic color purple.[2,3]

These color changes have been explained by the dye aggregation formed on biological substrates. The exciton coupling theory[4] states that the quantum mechanical resonance effects in a molecular dimer result in the splitting of the energy level of the monomer excited state into two levels, of which one is more stable and the other is less stable than the monomer. When dye molecules dimerize in a co-parallel arrangement, the electronic transition from the ground state to the less stable upper one is only allowed to give a hypsochromic shift of absorption. TB is known to have three characteristic absorption bands. In a dilute aqueous solution, TB concentration is within 10^{-5} to 10^{-6} mol L^{-1} and its absorption maximum appears at around 630 nm. This band, the α band, is believed to originate from the monomer. With an increase in TB concentration the α band shifts to the shorter wavelength region. This band is known as the β band. Further, the absorption peak shifts toward the shorter wavelength regions after adding agar. This is described as the γ band. The β and γ bands have been thought to be caused by the formation
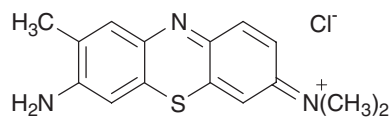

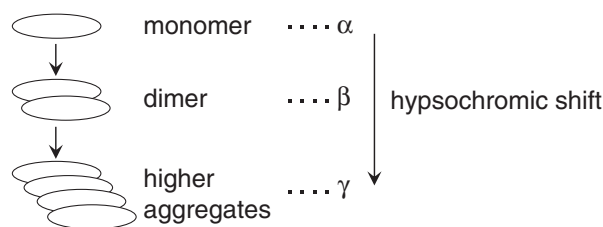**Figure 1.** Chemical structure of TB.

Figure 2. Schematic representation of aggregate structures of TB.

of dimers and higher molecular aggregates, respectively.[5] Figure 2 schematically illustrates aggregate structures of TB molecules corresponding to the metachromatic spectral bands. The metachromatic colors of TB observed in tissue staining are thus commonly thought to result from the aggregate formation of dye molecules bound to biological polymers having consecutively regular-spaced acid residues, for example, heparin and nucleic acids.[6–8] Based on this assignment, the correlation between the spectral shifts of TB with its concentration ratio to some stainable substrates had been stoichio-
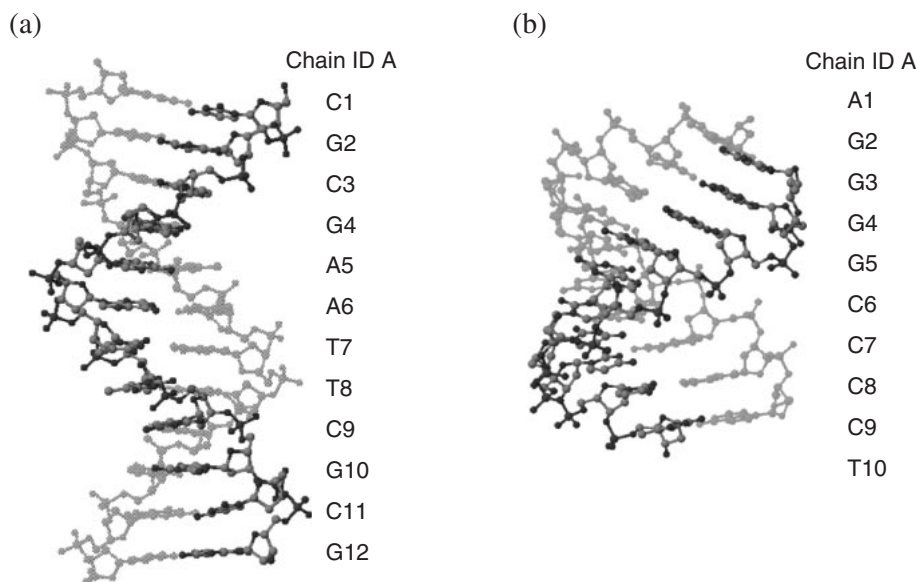
(a)

Chain ID A

C1
G2
C3
G4
A5
A6
T7
T8
C9
G10
C11
G12

(b)

Chain ID A

A1
G2
G3
G4
G5
C6
C7
C8
C9
T10

Figure 3. Crystal structure of the DNA oligomers. (a) d(CGCGAATTCGCG) is the B-form (PDB accession No. 1BNA) and (b) d(AGGGGCCCCT) is the A-form DNA (PDB accession No. 440D).

metrically investigated.[8–12] D'Ilario et al. observed in an aqueous solution the spectral changes in the absorption band of TB change with its concentration. They classified TB into six different aggregate species on the basis of the spectral changes.[13] However, both the aggregate structures and the mechanism of formation of TB aggregates on biomolecules have not been confirmed by any direct experimental observations. Despite many reported observations of TB metachromasy, there is little understanding of the metachromatic phenomena at the molecular level. Recently, TB staining has been expanded to detect apoptotic cells[14] and immature sperm cells,[15] by increase of nuclear staining. In these investigations, it is very important to comprehend the relationship between the metachromatic bands and chromatin condensation from the biological point of view. Nevertheless, discussions considering the metachromasy with structural or functional changes of the interacting biomolecules have been limited, because we still have little information on both the binding sites of TB on stainable substrates as well as the related aggregate structures. In this study, we observed TB metachromasy during nuclei staining; the complexes of TB with DNA were structurally studied by means of a computational approach focusing on the dimer formation in TB. Our examination is regarded as a first step in understanding of relationship between TB metachromasy and structure of biomolecules at the molecular level.

Experimental

Construction of the Complex Models. The structural models were constructed using the crystal structures of DNA obtained from Protein Data Bank and the optimized molecular structure of TB obtained from MO calculations. The crystal structures of the B- and A-form DNAs used in this simulation are shown in Figure 3. The B-form is well known to be a secondary structure of DNA in living cells.[16,17] In particular, oligomer (a), the dodecamer d(CGCGAATTCGCG),[18] has been widely used in experiments on the intermolecular interactions

between DNA and small molecules. This dodecamer is also known to have the typical helical parameters of B-DNA. To understand the effect of the helical structure of DNA on aggregate geometry, we also examined the A-form DNA oligomer (b), d(AGGGGCCCCT).[19] Since no crystallographic data are available on TB, we used its optimized molecular structure for model construction. The optimization was performed using the AM1 Hamiltonian.[20]

In the case of DNA staining by TB, many experimental data have suggested that TB binds to the phosphate group of DNA by electrostatic interaction.[1,9–12,21] TB is also well known as a metachromatic staining dye for other biomolecules with acidic residues.[6–8] For example, polysaccharides, such as heparin and hyaluronic acid, are stained matechromatically by TB.[6–8] Very large hypsochromic spectral shifts are observed in metachromatic TB staining of various substrates. This is also a very important factor for consideration of TB–DNA complexation. In order to form a higher aggregate of TB which results in a large hypsochromic spectral shift, a sufficient spatial area should be present around the target molecule. In this investigation therefore, a TB molecule is presumed to be bound with the phosphate residue of DNA in the fringed manner which was reported in many references,[6–12,21] although two binding manners, intercalation and groove binding, are well known for DNA complexation with an organic small molecule. The dimethyl amino group was assumed to bind to the phosphate group of DNA by electrostatic interaction. Because the basicity of dimethyl amino groups is higher than that of an unsubstituted amino group, a positive charge was assumed to be present on the nitrogen atom of the dimethyl amino group. Figure 4 illustrates two ways in which complexation between TB and DNA can occur. A single phosphate residue interacts with the dimethyl amino group in pattern I and the nitrogen in the dimethyl amino group is bound by two phosphate residues in pattern II. The geometry of the interaction between the dimethyl amino group and phosphate
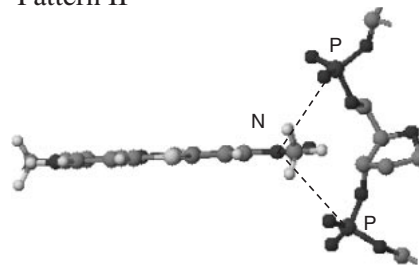
Pattern I
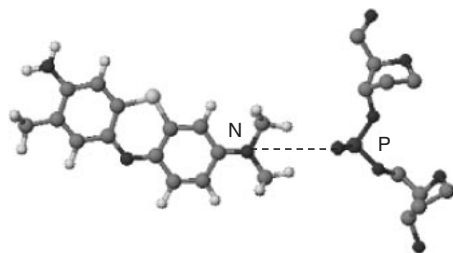
Pattern II

Figure 4. Two TB–DNA complexation patterns. TB:phosphate residue = 1:1 (pattern I) and TB:phosphate residue = 1:2 (pattern II).
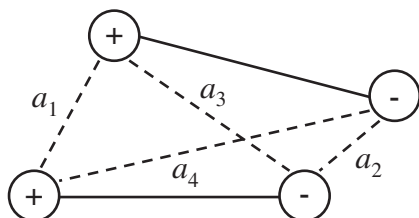

Figure 5. Extended-dipole model for estimating the exciton interaction.[26]

residues was determined on the basis of the reported structural data of some phosphates containing amino or dimethyl amino compounds.[22–25] TB molecules were arranged to make a nitrogen–phosphorus bond with a distance of 5 Å in consideration of steric interference between the substituents. These models are constructed on the assumption that there is no molecular structural change during the complexation. In the following section, to represent the TB dimers formed on the DNA oligomers, bound TB molecules are numbered in ascending order of the base sequence of chain ID A of the DNAs indicated in Figure 3 in each binding pattern.

Estimation of the Spectral Shifts. Exciton interaction was estimated using the extended-dipole model[26] to determine the effect of dye aggregation on spectral shift. Two adjacent TB molecules bound to DNA were considered as dimers in both cases. The energy shift from the calculated monomer absorption, ΔE, is given by the following eq 1.

$$\Delta E = \frac{|q|}{4\pi\varepsilon_0\varepsilon}\left[\frac{1}{a_1} + \frac{1}{a_2} - \frac{1}{a_3} - \frac{1}{a_4}\right] \qquad (1)$$

The molecules are replaced by transition dipoles of length l and charge $\pm q$. The transition moment M is assumed to be ql. The dipole moment of TB corresponding to absorption in the visible region was obtained using the INDO/S Hamiltonian.[27] The distances between the two poles a_1 to a_4 were determined by the geometric relationships between the dipole moments, as shown in Figure 5.

Results and Discussion

Dimer Formation on the B-Form DNA. Figures 6 and 7 show the calculated values of energy shift for the TB dimers formed with the B-DNA. For all the dimers, the interaction was calculated to be a positive value. This indicates that dimer formation causes a hypsochromic spectral shift from the monomer absorption. The reported metachromatic spectral
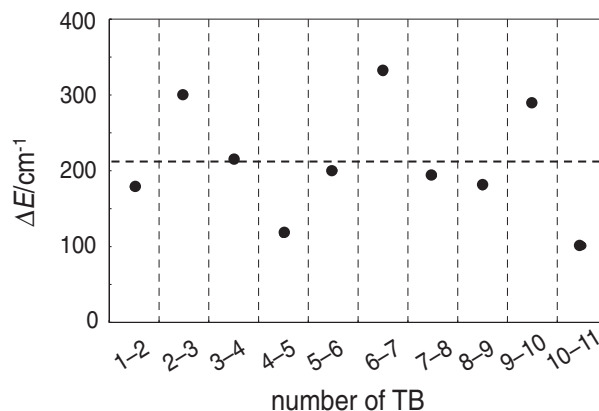

Figure 6. Calculated exciton interactions of TB for dimers formed on the B-DNA complex, based on pattern I (seen on Figure 4). The dotted line indicates the average of the ΔEs.
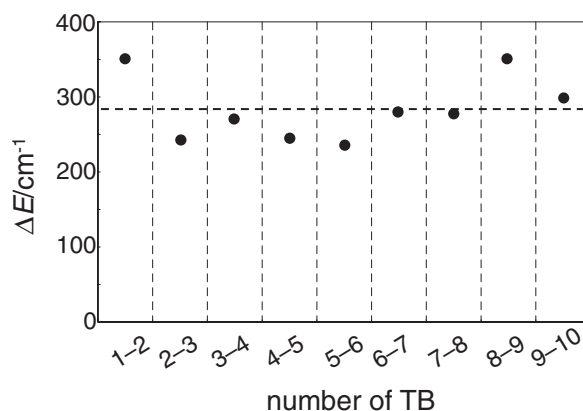

Figure 7. Calculated exciton interactions of TB for dimers formed on the B-DNA complex, based on pattern II (seen on Figure 4). The dotted line indicates the average of the ΔEs.

changes of TB and DNA in aqueous solutions are qualitatively supported by this result. The addition of DNA to an aqueous solution of TB was reported to cause a hypsochromic spectral shift, depending on the concentration of the phosphate residues of DNA in the solution.[9–12] Our result provides an insight into the ability of TB to form dimers with DNA by interacting with the phosphate residues of the B-DNA helix, resulting in the appearance of metachromatic colors. The metachromatic band
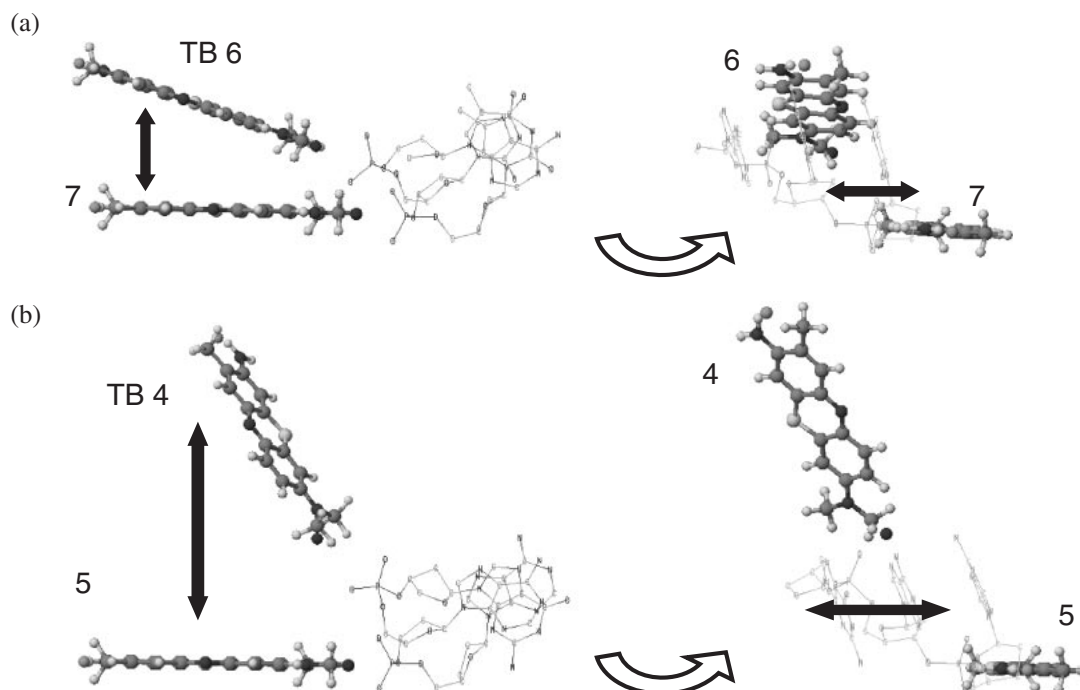
(a)

(b)

Figure 8. Comparison of the aggregation structure of TB in pattern I. The TB dimer (a) had a higher ΔE value than dimer (b).

of TB induced by DNA addition was reported to appear at around 580 nm; this corresponds to the β band, which shifts from the monomer band at around 630 nm. The calculated result shown Figures 6 and 7 is smaller than the experimental value. We calculated the values of spectral shift on a qualitative basis. This model is also based on a simple assumption in which the actual conformation of a DNA chain in a solution and the effects of other experimental conditions, such as pH and additives, are not taken into consideration.

Our calculation also revealed that the geometry of DNA is strongly related to the hypsochromic energy shift of TB. There was a distinct difference in the effect of DNA geometry between patterns I and II. In pattern I, we observed a difference in both the degree of overlap of planar TB molecules and the intermolecular distance between two TB molecules, as shown in Figure 8. Helical geometry and the sugar–phosphate backbone of DNA were considered to play a decisive role in determining these dimer arrangements. Among the many structural parameters that determine these two geometrical characteristics of DNA, we found the twist angle between the base pairs and the torsion angle of the phosphate group (α angle) (Table 1) to have a significant influence on the calculated spectral shift. The twist angle is regarded as representative of the helical geometry of DNA, because the difference in two consecutive twist angles (Δtwist) reflects the extent of helicity. The α torsional angle is defined as the angle of rotation of the P–O5′ bond of the sugar–phosphate backbone. The difference between neighboring α angles ($\Delta\alpha$) should be related to the difference between the directions of neighboring phosphate residues. We studied all the TB dimers with a difference in their twist and α angles and the corresponding energy shift. Table 1 shows four representative TB pairs. A relatively large Δtwist and a very small $\Delta\alpha$ were estimated for the pair 2–3. This structural characteristic reflects

Table 1. Relationship between ΔE Values of the Twist and α Angles for the Calculated TB Dimers in Pattern I

TB pair	$\|\Delta\text{twist}\|/°$	$\|\Delta\alpha\|/°$	$\Delta E/\text{cm}^{-1}$
2–3	13.68	0.25	300.59
4–5	5.55	30.24	116.92
6–7	0.63	2.54	330.44
9–10	11.38	6.58	290.36

the almost parallel arrangement of two TB molecules, which gives a large hypsochromic energy shift. When both Δtwist and $\Delta\alpha$ are very small like that in pair 6–7, we again obtained a large energy shift value. In the pattern I calculation, the pair 6–7, which has the most parallel dimer arrangement, showed the largest energy shift. As the calculation for pair 4–5 indicates, a considerably large $\Delta\alpha$ would be expected to cause low parallelism and distant arrangement of two TB molecules, and therefore a small metachromatic energy shift. The pair 9–10 also showed a large energy shift, comparable to that of pair 2–3 with its small $\Delta\alpha$. Figure 9 shows a plot of ΔE value versus $\Delta\alpha$. From these results, we can conclude that $\Delta\alpha$ is a key structural parameter for metachromatic spectral shift in pattern I complexation between TB and B-DNA.

In pattern II, we observed a small divergence in the calculated spectral shift as compared to that of pattern I (Figure 10). The average energy shift for all the molecular pairs
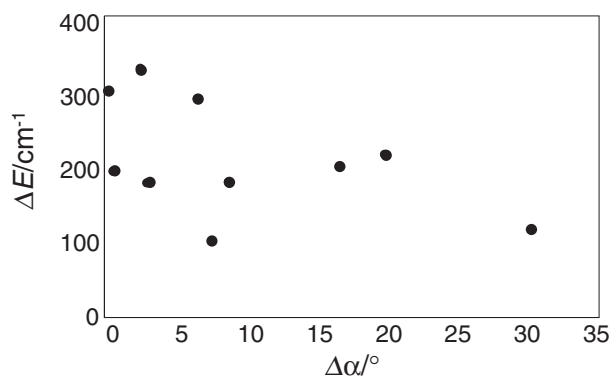
Figure 9. ΔE values for all TB dimers formed on the B-DNA in pattern I versus $\Delta\alpha$.
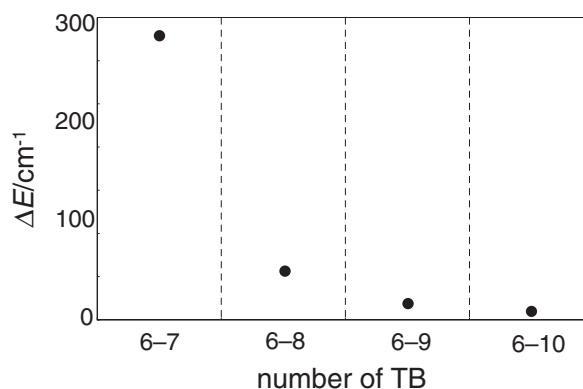

Figure 11.   Calculated exciton interactions of TB for dimers formed on four sets of binding sites in complexation pattern I.
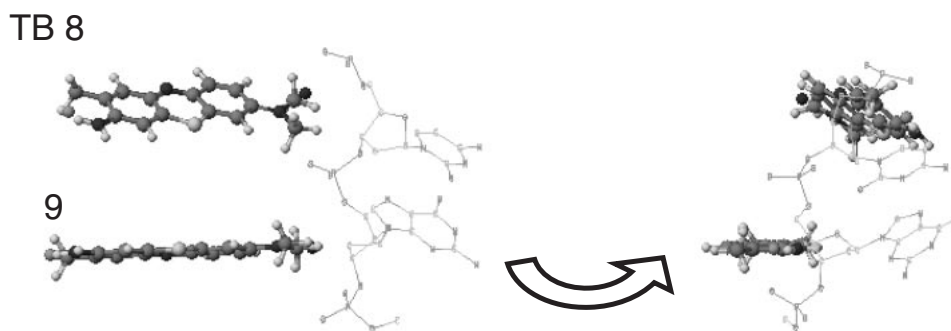

Figure 10.   TB dimer formation showed the highest ΔE value in complexation pattern II.

in pattern II is ca. $280\,\mathrm{cm}^{-1}$, which is about 1.3 times larger than that in pattern I. In pattern II, a significant relationship was not found between the helical structure of DNA and the calculated energy shifts. The narrow binding site in pattern II limits the ability of TB molecules to bind with the DNA chain in a configuration that is almost parallel to the molecular plane of the base pair. This structural limitation should result in the overlap of neighboring TB molecules in the TB–DNA complex. TB dimer geometry yielded a large energy shift not dependent on the $\Delta\alpha$ of the DNA. In many stoichiometric experiments on the metachromasy of TB and DNA, the metachromatic spectral changes induced by DNA addition were reported to occur when the concentration ratio of DNA to TB was 0.5 to 1.0.[9–12] There is no significant difference in the shape of the reported metachromatic β bands. These observations suggested that the almost identical aggregate structure of TB is a major component of the bands in various concentrations. The metachromatic spectral shift was believed to originate from the dimers formed on the binding sites neighboring those in pattern I (Figure 11). When the concentration ratio of TB to DNA is smaller than the equimolar ratio, the number of metachromatic dye dimers of TB bound to DNA will decrease as per pattern I, because unoccupied binding sites are considered to be present in the TB–DNA complex. On the other hand, pattern II gives an almost uniform geometry of TB dimers under the appropriate concentrations. Although the reported experimental results can be explained by both complexation patterns between TB and DNA, our results indicate that pattern II is more plausible than pattern I.

The hypsochromic energy shifts of absorption band due to the dimerization of TB were calculated in this examination. However, the TB dimer geometry shows not only parallel stacking of molecular planes but twisted forms. In the case of a twisted dimer, a strict symmetric limitation is broken to allow the weak bathochromic transition. This is considered to reflect the broadening of metachromatic band to longer wavelength region over the monomer band observed in absorption spectra of TB with DNA in solution.[12]

Wang et al. studied CD spectra of TB solutions with addition of different amounts of calf thymus DNA.[28] They suggested multiple binding modes of TB to DNA affected by their concentration ratio. At low concentration ratio, TB molecules partially intercalated into DNA base pairs, while at high ratio, TB molecules stacked along the helix surface. In an actual staining state, as their result indicated, there are many ways of possible dimeric arrangements of TB on DNA chains. Our TB–DNA complex models are based on the simple assumption, however the models could explain spectral features of TB and help in understanding the metachromatic phenomena.

Calculation results also provided us with a clue for studying the metachromatic spectral changes resulting from the formation of higher aggregates of TB. As mentioned in the introduction, the formation of higher aggregates of TB is commonly considered to be the origin of the γ band observed in the shorter wavelength region and not the dimer band. All the calculated results showed a hypsochromic energy shift in both patterns. This clearly indicates that the formation of a TB

trimer or a higher aggregate results in a larger energy shift than the formation of the dimers, that is, higher aggregates bring about a large hypsochromic spectral shift.

We obtained an similar result when examining the dimer formation of TB with some other B-form DNAs.[29–34] It was found that the TB dimer structure formed on the DNA chain reflects the backbone geometry of B-form DNA. This investigation only provides us with a qualitative description of the formation of a metachromatic dimer of TB and B-DNA. This however, clarifies an important concept that the phosphate residues of B-DNA can function as a TB binding site to form a metachomatic dye dimer.

Complexation with A-Form DNA. Our experiments on the complex formation of TB with several B-DNA oligomers indicate that various dimer geometries can result depending on the helical characteristics of DNA, particularly the conformation of the phosphate residues. In biosystems however, the helical conformation of DNA changes because of its interactions with other biomolecules or under various ambient conditions. A-type DNA was then examined because it has an atypical helical property. The B-type helix is the main DNA conformation in biosystems however, the A-form is also important because of its biological importance. The long GC stretches in a DNA chain has been known to favor the A-conformation.[35] In addition, the complexes of DNA with some proteins are thought to induce partial transformation from the B- to the A-type, and this is associated with the global bending of DNA.[36] Our study of A-DNA provides information regarding the relationship between the structure and staining color of biomacromolecules in actual staining processes. A-DNA is characterized by a tight helix and a deep and narrow major groove. This structural feature correlates well with the deoxyribose sugar pucker conformation. In A-DNA, the pucker conformation is observed at C3′-*endo*, resulting in a short distance between the neighboring phosphate residues.[9] In addition, the O–P–O plane of the phosphate residues is almost parallel to the stacking direction of the base pairs. These two local features basically made the complexation of a TB molecule with the A-DNA improbable in both patterns. Figure 12 illustrates impossible complexation of a TB molecule and the A-form DNA. There is no sufficient space for a TB molecule to bind with the A-form DNA in the present binding mode and a TB molecule was found to collide with the DNA strand in many binding positions as shown in Figure 12. Therefore, TB dimer formation is very problematic as well.

Conclusion

This paper focused on the dimer structure of TB molecules formed on DNA strands. TB molecules bound to the phosphate residues of B-DNA could form dimers that bring about a hypsochromic shift from the monomer absorption. The present results also suggest the possibility of formation of higher aggregates. Two complexation patterns were examined in our simulation, and the dimer structures of TB formed in both these patterns had a different sensitivity to the helical parameters of DNA. In both complexation patterns, not all the phosphate residues in A-form DNA could be regarded as binding sites for TB. Our study indicated that the formation of TB aggregates is
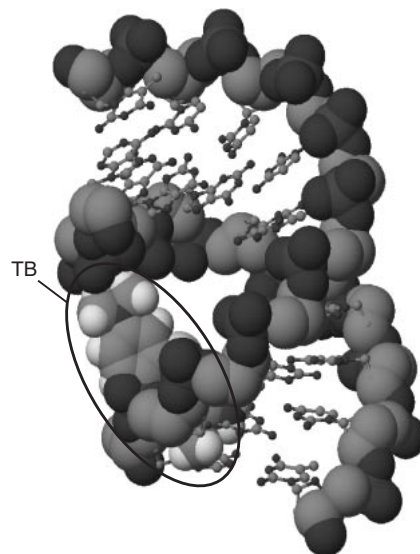

Figure 12. This figure shows impossible complexation of a TB molecule and the A-form DNA. Structural characteristics of A-DNA lead to steric hindrance in biding sites to DNA strands.

strongly influenced by the helical geometry of DNA. These results help in understanding the color change observed in the metachromatic staining of some tissue elements.

References

1 J. A. Bergeron, M. Singer, *J. Biophys. Biochem. Cytol.* **1958**, *4*, 433.

2 J. F. A. McManus, R. W. Mowray, *Staining Methods*, Harper & Brothers, New York, **1960**.

3 H. H. Niebel, B. Chomet, *J. Am. Dent. Assoc., JADA* **1964**, *68*, 801.

4 K. Kasha, *Spectroscopy of the Excited State*, Plenum Press, New York, **1976**.

5 L. Michaelis, S. Granick, *J. Am. Chem. Soc.* **1945**, *67*, 1212.

6 L. Lison, *Histochimie et Cytochimie Animates*, Gauthier-Villars, **1960**.

7 T. Kunio, *Med. Technol.* **1987**, *15*, 409.

8 N. C. Mandal, B. B. Biswas, M. K. Pal, *Histochemie* **1969**, *18*, 202.

9 A. Levine, M. Schubert, *J. Am. Chem. Soc.* **1952**, *74*, 91.

10 D. F. Bradley, M. K. Wolf, *Proc. Natl. Acad. Sci. U.S.A.* **1959**, *45*, 944.

11 M. E. Lamm, L. Childers, M. K. Wolf, *J. Cell Biol.* **1965**, *27*, 313.

12 Y. Huse, K. Miyaki, M. Tsuboi, *Bull. Chem. Soc. Jpn.* **1965**, *38*, 1039.

13 L. D'Ilario, A. Martinelli, *Modell. Simul. Mater. Sci. Eng.* **2006**, *14*, 581.

14 J. Erenpreisa, T. Freivalds, H. Roach, R. Alston, *Histochem. Cell Biol.* **1997**, *108*, 67.

15 J. Erenpreiss, K. Jepson, A. Giwercman, I. Tsarev, J. Erenpreisa, M. Spano, *Hum. Reprod.* **2004**, *19*, 2277.

16 W. Saenger, *Peinciples of Nucleic Acid Structure*, Springer, New York, **1984**.

17 R. L. P. Adams, J. T. Knownler, D. P. Leader, *The*

Biochemistry of Nucleic Acids, 11th ed., Chapman & Hall, London, **1992**.

18   H. R. Drew, R. M. Wing, T. Takano, C. Broka, S. Tanaka, K. Itakura, R. E. Dickerson, *Proc. Natl. Acad. Sci. U.S.A.* **1981**, *78*, 2179.

19   Y.-G. Gao, H. Robinson, A. H.-J. Wang, *Eur. J. Biochem.* **1999**, *261*, 413.

20   M. J. S. Dewar, E. G. Zoebisch, E. F. Healy, J. J. P. Stewart, *J. Am. Chem. Soc.* **1985**, *107*, 3902.

21   J. Erenpreisa, T. Freivalds, *Folia Histochem. Cytochem.* **1979**, *17*, 93.

22   R. G. Ball, R. M. Elofson, *Can. J. Chem.* **1985**, *63*, 332.

23   I. Halasz, K. Lukic, H. Vancik, *Acta Crystallogr., Sect. C* **2007**, *63*, o61.

24   A. K. Idrissi, M. Saadi, M. Rafiq, E. M. Holt, *Acta Crystallogr., Sect. C* **2002**, *58*, o604.

25   J. A. Paixão, A. Matos Beja, M. Ramos Silva, J. Martin-Gil, *Acta Crystallogr., Sect. C* **2000**, *56*, 1132.

26   V. Czikklely, H. D. Forsterling, H. Kuhn, *Chem. Phys. Lett.* **1970**, *6*, 207.

27   M. C. Zerner, G. H. Loew, R. F. Kirchner, U. T. Mueller-Westerhoff, *J. Am. Chem. Soc.* **1980**, *102*, 589.

28   J. Wang, X. Yang, *Spectrochim. Acta, Part A* **2009**, *74*, 421.

29   K. J. Edwards, D. G. Brown, N. Spink, J. V. Skelly, S. Neidle, *J. Mol. Biol.* **1992**, *226*, 1161.

30   H. Yuan, J. Quintana, R. E. Dickerson, *Biochemistry* **1992**, *31*, 8009.

31   T. A. Larsen, M. L. Kopka, R. E. Dickerson, *Biochemistry* **1991**, *30*, 4443.

32   D. R. Mack, T. K. Chiu, R. E. Dickerson, *J. Mol. Biol.* **2001**, *312*, 1037.

33   G. G. Prive, K. Yanagi, R. E. Dickerson, *J. Mol. Biol.* **1991**, *217*, 177.

34   J. Hizver, H. Rozenberg, F. Frolow, D. Rabinovich, Z. Shakked, *Proc. Natl. Acad. Sci. U.S.A.* **2001**, *98*, 8490.

35   H.-L. Ng, R. E. Dickerson, *Nucleic Acids Res.* **2002**, *30*, 4061.

36   X.-J. Lu, Z. Shakked, W. K. Olson, *J. Mol. Biol.* **2000**, *300*, 819.